Hydrogeology Journal – Electronic Supplementary Material

A density-dependent multi-species model to assess groundwater flow and nutrient transport in the coastal Keauhou aquifer, Hawai‘i, USA

Brytne K. Okuhata[1*], Aly I. El-Kadi [1, 2], Henrietta Dulai[1, 2], Jonghyun Lee[2, 3], Christopher A. Wada[2, 4], Leah L. Bremer[2, 4], Kimberly M. Burnett [2, 4], Jade M.S. Delevaux [5], Christopher K. Shuler [2]

1. Department of Earth Sciences, University of Hawai‘i at Mānoa, Honolulu, HI 96822, USA
2. Water Resources Research Center, University of Hawai‘i at Mānoa, Honolulu, HI 96822, USA
3. Department of Civil and Environmental Engineering, University of Hawai‘i at Mānoa, Honolulu, HI 96822, USA
4. University of Hawai‘i Economic Research Organization, Honolulu, HI 96822, USA
5. The Natural Capital Project, Stanford University, Stanford, California 94305-5020, USA

* corresponding author: bokuhata@hawaii.edu

S.1 - Data of sampled measurements used for model calibration.

Table S1.1 $\delta^{15}N$ measurements for wells and submarine springs.

Sample	Well ID	Latitude	Longitude	Sample depth (m msl)	$\delta^{15}N$ (‰)	$\delta^{18}O$ (‰)
HR2	8-4459-001	19.74	-155.98	-4.51	1.83	0.35
NELHA 3A	8-4363-022	19.72	-156.05	-2.74	3.59	3.67
Kohanaiki 5	8-4161-006	19.69	-156.03	-2.56	3.59	0.27
Kohanaiki 7	8-4161-008	19.69	-156.03	-1.52	3.61	0.25
Kohanaiki 6	8-4161-007	19.69	-156.03	-2.59	3.76	0.29
NELHA 9A	8-4262-005	19.71	-156.04	-16.76	6.24	0.77
Kahaluu Shaft	8-3557-005	19.58	-155.95	-2.29	1.72	0.68
Keopu 2	8-3858-002	19.64	-155.96	-133.67	1.87	-0.35
Kahaluu C	8-3557-003	19.58	-155.94	-8.83	1.89	0.87
Kahaluu B	8-3557-002	19.58	-155.95	-11.28	2.15	0.35
Kahaluu D	8-3557-004	19.58	-155.94	-5.60	2.17	0.12
Holualoa	8-3657-001	19.61	-155.95	-13.72	3.07	0.84
HHA7	-	19.66	-156.02	0	10.00	5.00
HHB3	-	19.66	-156.02	0	21.60	11.40
P24	-	19.78	-156.04	0	2.10	-0.10
PKI1	-	19.69	-156.03	0	3.50	0.30
PKI2	-	19.69	-156.03	0	3.60	0.20
P37	-	19.63	-155.99	0	2.10	-0.10
Heiau 1	-	19.57	-155.96	0	2.80	0.70
Heiau 2	-	19.57	-155.96	0	3.10	0.80
Heiau 3	-	19.57	-155.96	0	3.40	1.40
P39	-	19.63	-155.99	0	4.90	1.50
OKA2	-	19.64	-156.01	0	5.50	1.90
P34	-	19.64	-156.01	0	6.40	1.70
P40	-	19.62	-155.98	0	6.40	1.80

Table S1.2 Median salinity, nitrate+nitrite, and phosphate measurements at wells used for calibration (original data from Tachera 2021). Samples marked with * indicate basal measurements used to compute the boundary condition concentration. Samples marked with + indicate high-level measurements used to compute the boundary condition concentration, but were not used in model calibration.

Sample	Well ID	Longitude	Latitude	Salinity	Nitrate+Nitrite (mg/L)	Phosphate (mg/L)
NELHA 1	8-2979-011	-156.03	19.71	11.33	1.17	0.102
Kahaluu DW	8-3457-004	-155.95	19.57	1.6	0.05	0.04
*Kahaluu B	8-3557-002	-155.95	19.58	0.46	1.18	0.14
*Kahaluu C	8-3557-003	-155.94	19.58	0.15	1.22	0.14
*Kahaluu D	8-3557-004	-155.94	19.58	0.44	1.14	0.15
Kahaluu Shaft	8-3557-005	-155.95	19.58	0.72	1.23	0.13
*Holualoa	8-3657-001	-155.95	19.61	0.43	1.11	0.12
Keopu 1	8-3858-001	-155.96	19.64	0.98	0.01	0.01
Keopu 2	8-3858-002	-155.96	19.64	0.1	1.0	0.14
Kohanaiki 4	8-4161-005	-156.03	19.69	8.25	1.15	0.10
Kohanaiki 5	8-4161-006	-156.03	19.69	8.61	1.35	0.10
Kohanaiki 6	8-4161-007	-156.03	19.69	8.32	1.15	0.10
Kohanaiki 7	8-4161-008	-156.03	19.69	8.45	1.12	0.12
Kohanaiki 2	8-4262-002	-156.03	19.70	9.14	1.06	0.12
NELHA 9A	8-4262-005	-156.04	19.71	20.36	1.03	0.10
NELHA 3A	8-4363-022	-156.05	19.72	8.22	1.50	0.11
*Makalei	8-4458-002	-155.97	19.73	0.68	0.63	0.21
HR2	8-4459-001	-155.98	19.74	0.64	0.77	0.28
HR4	8-4459-002	-155.98	19.74	0.68	0.65	0.33
NELHA 12A	8-4463-006	-156.05	19.74	22.14	0.43	0.10
+Honokohau Deepwell	8-4158-002	-155.96	19.68	0.12	1.12	0.12
+Kalaoa Deepwell	8-4358-001	-155.97	19.71	0.12	0.96	0.13
+Keopu Deepwell	8-3957-001	-155.95	19.65	0.06	1.10	0.12
+Palani Ranch Deepwell	8-4158-003	-155.96	19.69	0.09	0.99	0.14
+QLT Deepwell	8-4057-001	-155.95	19.66	0.08	1.21	0.12

Table S1.3 Salinity, nitrate+nitrite, and phosphate measurements at submarine springs used for calibration.

Sample	Longitude	Latitude	Salinity	Nitrate+Nitrite (mg/L)	Phosphate (mg/L)
P23	-156.03	19.78	-	0.50	0.02
P24	-156.04	19.78	-	0.18	0.19
P25	-156.05	19.73	-	0.32	0.64
PKI2	-156.03	19.69	16.12	1.06	0.13
PKI1	-156.03	19.69	15.06	1.05	0.12
HHA7	-156.02	19.66	20.98	0.95	0.13
HHB3	-156.02	19.66	22.85	1.64	0.1
QLT1	-156.02	19.64	-	0.23	0.19
P34	-156.01	19.64	23.72	0.79	0.08
OKA2	-156.01	19.64	31.2	0.20	0.05
P37	-155.99	19.63	-	0.18	0.12
P38	-155.99	19.64	16.58	0.51	0.11
P39	-155.99	19.63	11.74	0.93	0.04
P40	-155.98	19.62	12.8	1.40	0.04
P41	-155.97	19.60	-	0.42	0.09
P43	-155.96	19.58	16.77	0.50	0.08
Heiau 1	-155.96	19.57	4.53	1.40	0.08
Heiau 2	-155.96	19.57	4.43	1.45	0.04
Heiau 3	-155.96	19.57	6.63	1.27	0.07

As most water level measurements are obtained during the drilling process, head data used for model calibration are static values. In general, the static head measurements are within fluctuations, as demonstrated in Fig. S1. The static measurements from four monitoring wells fall within the range of transient water level measurements that are continuously monitored on a quarterly basis.

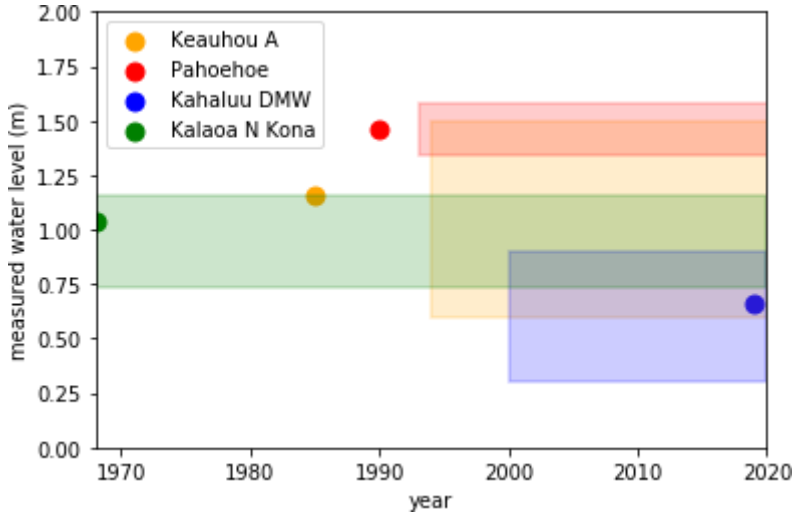

Fig. S1 Comparison of long-term water level changes versus static measurements used for model calibration. Colored boxes represent range of water levels measured within each well, as documented by the Commission on Water Resource Management (State of Hawai‘i 2021). Colored circles represent static measurements, all of which fall within the corresponding ranges

S.2 – Classifications and characteristics of on-site sewage disposal systems (OSDS) within the Keauhou basal aquifer study area.

Table S2 Typical OSDS class effluent concentrations (based on Whittier and El-Kadi 2014).

OSDS Class	Treatment	Typical N conc. [mg/L]	Typical P conc. [mg/L]	Total quantity (within study area)
I	Soil	1	<2	1094
II	Septic tank to seepage pit	39-82	11-22	77
III	Aerobic treatment to seepage pit	7-60	2-18	16
IV	Cesspool	15-90	5-20	6251

S.3 – Sensitivity Analysis

Due to the extreme hydrogeologic heterogeneity observed across the islands and the lack of hydrogeologic data in this specific study area, four flow and transport parameters were tested to determine which is the most influential during the model calibration process. The primary flow parameters tested were K_h and K_h/K_v, while the primary transport parameters tested were φ and α_L. To maintain consistency for sensitivity analyses, all four of the flow and transport parameters were multiplied by factors of 0.5 and 2.0. Apart from the parameter tested, all others remained fixed at the values used for the control model. The relative sensitivity coefficient, *S*, was computed following the equation (Nearing et al. 1990):

$$S = \frac{\left[\frac{(O_2 - O_1)}{O_{\text{avg}}}\right]}{\left[\frac{(I_2 - I_1)}{I_{\text{avg}}}\right]} \quad \text{(S1)}$$

where I_2 and I_1 are the highest and lowest model input parameter values, respectively, and I_{avg} is the average of the two *I* values. Similarly, O_2 and O_1 are the highest and lowest output values respective to the input values, and O_{avg} is the average of the two *O* values. Following a similar method performed by Shuler et al. (2017), the root-mean-square error (RMSE) computed from head, salinity, N, and P concentrations in wells were used as the respective *O* variables to investigate how changes in parameters can improve or degrade model calibration. In this way, the sensitivity of an identified parameter can be quantified with a range of validity. The final *S* is therefore normalized and can thus be compared across parameters (Nearing et al. 1990). This assessment can identify which parameters were critical for calibration and should be further investigated.

Sensitivity analysis showed that all four calibration variables (head, salinity, N, and P) are most significantly affected by the assigned upland boundary flux, as illustrated by the sensitivity coefficients in Fig. S3. Head results were expectedly sensitive to change in the boundary flux. The specified N and P concentrations assigned to the upland boundary were not altered during this analysis, so as anticipated, a reduced boundary flux resulted in higher N and P concentrations simulated in wells relative to the control model, due to reduced dilution. In contrast, relatively lower N and P concentrations resulted under increased flux, which seemed to improve the accuracy of calibration with a lower RMSE.

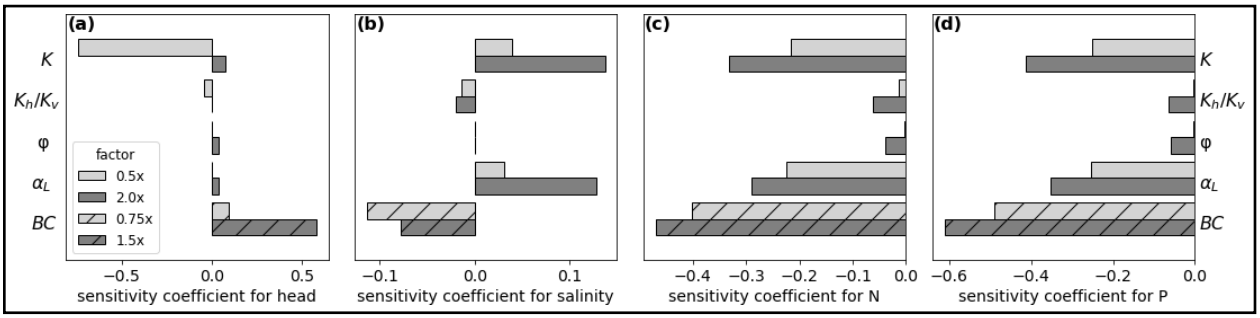

Fig. S3 Sensitivity coefficients, *S*, for select model parameters (K_h, hydraulic conductivity; K_h/K_v, vertical anisotropy; φ, porosity; α_L, longitudinal dispersivity; BC, upland boundary condition). Coefficients were computed using RMSE values between measured and simulated (a) head levels, (b) salinity, (c) N concentrations, and (d) P concentrations in wells with respect to a factor change in each parameter input value. The control values for K_h, K_h/K_v, φ, α_L, and BC were 2500 m/d, 200, 0.1, 25 m, 388,399 m^3/d, respectively. Note different scales on charts.

Among flow and transport parameters, calibration accuracy was most significantly affected by α_L and K_h (Fig. S3). A higher α_L value produced an overall narrower range of simulated N and P concentrations. This therefore reduced the calibration error of concentrations that were associated with the original model calibration. The higher α_L, however, also produced slightly more scatter amongst values with lower simulated concentrations. These results suggest the heterogeneous nature of α_L, which was not simulated in the model. The primary parameter that impacted head calibration was K_h. Varying the K_h most significantly affected the calibration accuracy of wells with higher hydraulic head measurements, which are generally distanced from the coastal wells. These wells may also be affected by the Hualālai rift zone, of which the geological nature is currently not well characterized. Wells with higher simulated nutrient concentrations were also significantly impacted by K_h. As K_h increased, the simulated nutrient concentrations decreased, likely due to the higher flux of water that moved through the model.

S.4 – Results obtained using a heterogeneous hydraulic conductivity distribution produced from automated calibration

Potential improvements in model results were investigated by calibrating K_h utilizing PCGA, which produced a heterogeneous field with values that ranged from approximately 75 to 4,000 m/d (Fig. S4). Accuracy of salinity calibration in wells improved from a baseline of about 9 to about 3 for the RMSE, but slightly reduced the RMSE of hydraulic head from 0.39 to 0.72 m. Additionally, N and P concentration calibration accuracy worsened. Compared to baseline RMSE values, the RMSE values for N concentrations in wells and submarine springs were 1.15 and 3.06 mg/L, respectively, while the RMSE values for P concentrations in wells and submarine springs were 0.28 and 0.88 mg/L, respectively. A primary reason for the inaccuracies is due to the salinity profile of the Keopu 2 deep monitoring well. A second layer of fresh water exists, that is located approximately 180-340 m below msl (Fukunaga & Associates, Inc. 2017). Such a profile is not considered in the current model, and therefore necessitates the use of a very low calibrated K_h surrounding the well to simulate the lower salinity concentrations. Removing this observation from the error assessment would reduce the baseline salinity RMSE from 9.16 to 5.24. These PCGA calibration results demonstrate the need to further investigate these layered fresh and saline groundwaters. Similar layered groundwater systems have also been discovered on the east side of Hawai‘i Island (Thomas et al. 1996), suggesting the prominence of these features.

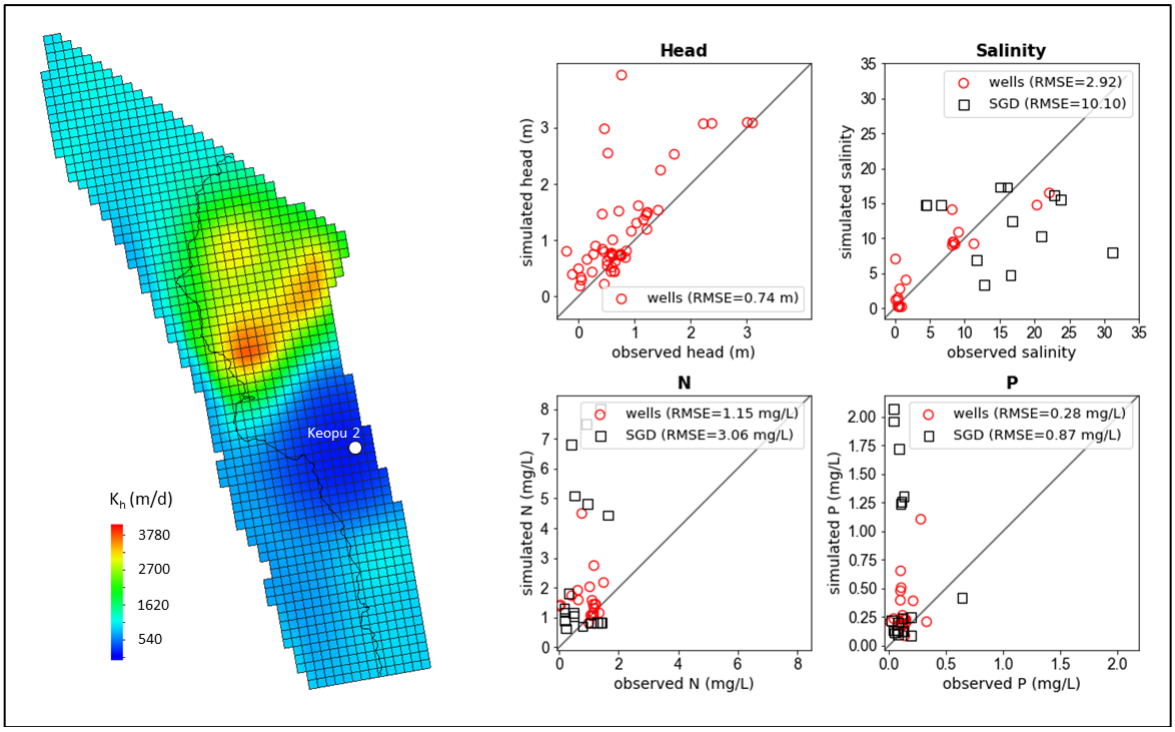

Fig. S4 Calibration of K_h at approximately -2 m msl depth (model layer 2) using PCGA (Lee et al. 2016). White circle marker indicates the location of Keopu 2 deep monitoring well. Scatter plots show calibration results between observed and simulated head, salinity, N concentrations, and P concentrations at wells and submarine springs using heterogeneous K_h distribution.

References cited in ESM

Fukunaga & Associates, Inc. (2017) Hawaii County Water Use and Development Plan Update: Keauhou Aquifer System. https://www.hawaiidws.org/wp-content/uploads/2018/06/Combined-Ph-1-2-Keauhou-20170510_w-Appendix-final.pdf. Accessed 8 October 2020.

Kitanidis PK (1996) On the geostatistical approach to the inverse problem. Adv. Water Res. 19(6):333-342, doi 10.1016/0309-1708(96)00005-X

Lee J, Kitanidis PK (2014) Large-scale hydraulic tomography and joint inversion of head and tracer data using the Principal Component Geostatistical Approach (PCGA). Water Resour. Res. 50(7):5410-5427, doi 10.1002/2014WR015483

Lee J, Yoon H, Kitanidis PK, Werth CJ, Valocchi AJ (2016) Scalable subsurface inverse modeling of huge data sets with an application to tracer concentration breakthrough data from magnetic resonance imaging. Water Resour. Res. 52(7):5213-5231, doi 10.1002/2015WR018483

Nearing MA, Deer-Ascough L, Laflen JM (1990) Sensitivity analysis of the WEPP hillslope profile erosion model, Trans. ASAE 33(3):839-0849, doi 10.13031/2013.31409

Shuler CK, El-Kadi AI, Dulai H, Glenn CR, Fackrell J (2017) Source partitioning of anthropogenic groundwater nitrogen in a mixed-use landscape, Tutuila, American Samoa, Hydrogeol. J. 25(8):2419-2434, doi 10.1007/s10040-017-1617-x

State of Hawaii (2021) Monitoring Data. http://dlnr.hawaii.gov/cwrm/groundwater/monitoring/. Accessed 2021.

Tachera D (2021) Groundwater chemistry: Nutrient Data, HydroShare, https://doi.org/10.4211/hs.d812bbb7c93348999371c9f1f517297f

Thomas DM, Paillet FL, Conrad ME (1996) Hydrogeology of the Hawaii Scientific Drilling Project borehole KP-1 2. Groundwater geochemistry and regional flow patterns, J. Geophys. Res. 101(B5), 11: 683-11,694, doi 10.1029/95JB03845

Whittier RB, El-Kadi AI (2014) Human health and environmental risk ranking of on-site sewage disposal systems for the Hawaiian Islands of Kauai, Molokai, and Hawaii. Final Rep Prep State Hawaii Dep Health Safe Drink Water Branch. https://health.hawaii.gov/wastewater/files/2015/09/OSDS_NI.pdf. Accessed 25 September 2020.